# Thresholds for Paleozoic ice sheet initiation

D.P. Lowry[1]*, C.J. Poulsen[1], D.E. Horton[2], T.H. Torsvik[3], and D. Pollard[4]
[1]Department of Earth and Environmental Sciences, University of Michigan, Ann Arbor, Michigan 48109, USA
[2]Department of Environmental Earth System Science, Stanford University, Stanford, California 94305, USA
[3]Centre for Earth Evolution and Dynamics, University of Oslo, Oslo 0316, Norway
[4]Earth and Environmental Systems Institute, Pennsylvania State University, University Park, Pennsylvania 16802, USA

## ABSTRACT

**Continental drift and atmospheric greenhouse gas concentrations have each, in turn, been proposed to explain the evolution of Paleozoic climate from early era ice-free conditions to late era continental-scale glaciation, despite continually increasing solar luminosity. To assess the relative roles of continental configuration and atmospheric $pCO_2$ on the formation of continental-scale ice sheets, we use a coupled ice sheet–climate model to simulate ice sheet initiation at eight different Paleozoic time slices using uniform topography. For each time slice, we simulate the climate at three atmospheric $pCO_2$ levels (560, 840, and 1120 ppm) and both constant (97.5% of modern) and time-appropriate solar luminosity values. Under constant luminosity, our results indicate that continental configurations favor ice sheet initiation in the mid-Paleozoic (400–340 Ma). After accounting for solar brightening, ice sheet initiation is favored in the early Paleozoic (480–370 Ma) simulations. Neither of these results is consistent with geological evidence of continental-scale glaciation. Changes in atmospheric $pCO_2$ can reconcile these differences. Sufficiently high (≥1120 ppm) or low (≤560 ppm) $pCO_2$ overcomes paleogeographic and luminosity predispositions to ice-free or ice age conditions. Based on our simulations and geological evidence of glaciation and atmospheric composition, we conclude that atmospheric $pCO_2$ was the primary control on Paleozoic continental-scale glaciation, while paleogeographic configurations and solar irradiance were of secondary importance.**

## INTRODUCTION

Continental-scale glaciation has been absent throughout the majority of the Phanerozoic, interrupted by just two long-lasting (>10 m.y.) ice ages in the late Paleozoic and late Cenozoic, and multiple short-lived glaciations (<10 m.y.) in the Late Ordovician, Late Devonian, and early Carboniferous (Kennett, 1977; Caputo and Crowell, 1985; Brenchley et al., 2003; Montañez and Poulsen, 2013). The absence of evidence for continental-scale glaciation during most of the Phanerozoic suggests that cold climate states have been relatively rare. The primary drivers of Phanerozoic continental glaciation are hypothesized to involve continental drift and the long-term evolution of atmospheric $pCO_2$ and solar irradiance (e.g., Kennett, 1977; Crowley and Baum, 1992; Herrmann et al., 2003; Horton et al., 2007; Finnegan et al., 2011; Montañez and Poulsen, 2013).

The relative contributions of these drivers to Paleozoic climate states remain uncertain. Paleogeographic reconstructions indicate that during the early Paleozoic Gondwana migrated southward to higher latitudes (and lower insolation), and was centered over the austral pole throughout the Devonian and early Carboniferous (Cocks and Torsvik, 2002; Torsvik and Cocks, 2004). Despite the polar location of the continental landmass, glaciogenic evidence from this interval is scarce in the geologic record, suggesting that continental ice sheets were largely absent (Caputo and Crowell, 1985). In contrast, the northward migration of parts of Gondwana, including modern-day Africa, South America, and Arabia, toward lower latitudes (and greater insolation) and collision with northern Laurasia coincided with the onset of the late Paleozoic ice age (LPIA) (Torsvik and Cocks, 2004; Fielding et al., 2008; Montañez and Poulsen, 2013). Variations in atmospheric $pCO_2$ may provide a more satisfying explanation; however, both the Paleozoic record of $pCO_2$ and the concentrations required to initiate continental-scale glaciation during times of varying solar irradiance and paleogeography are poorly constrained.

The goal of this study is to investigate the conditions under which ice sheet growth initiated during the Paleozoic Era through the use of coupled climate–ice sheet simulations. We specifically address the influence of continental landmass configurations on glacial inception and the effect of landmass configuration and solar luminosity on $pCO_2$ thresholds for glaciation.

## METHODS

We use the GENESIS version 3.0 general circulation model (GCM) coupled to BIOME4, an equilibrium vegetation model, and a three-dimensional dynamic ice sheet model to simulate a series of time slices in the late Paleozoic (see the GSA Data Repository[1]). GENESIS is composed of an atmospheric GCM (AGCM) coupled to both a land-surface model and a slab ocean model with diffusive heat transport. The AGCM has a T31 (3.75° × 3.75°) spectral resolution with 18 vertical levels, while the land-surface grid has a 2° × 2° resolution (Alder et al., 2011).

We conducted two sets of experiments, each using continental configurations from eight different Paleozoic time periods, including the Early Ordovician (480 Ma), early Silurian (440 Ma), Early Devonian (400 Ma), Late Devonian (370 Ma), early Carboniferous (340 Ma), late Carboniferous (310 Ma), early Permian (280 Ma), and Early Triassic (250 Ma) (Fig. 1; Cocks and Torsvik, 2002; Torsvik and Cocks, 2004). In the first set of experiments, we varied atmospheric $pCO_2$ between pre-industrial levels: 560 (2× $CO_2$), 840 (3× $CO_2$), and 1120 ppm (4× $CO_2$), but kept solar luminosity at 1330.9 $Wm^{-2}$, or 2.5% less than present, a value appropriate for the late Paleozoic. We used an asynchronous coupling technique, which consisted of alternating integrations of the AGCM and ice-sheet model, following methods presented in Herrington and Poulsen (2012; see the Data Repository). After 5000 yr of asynchronous coupling, we then ran the ice sheet model an additional 45,000 yr to estimate an equilibrium volume.

In the second set of experiments we investigated the influence of solar luminosity on glacial inception, using a methodology slightly modified from that employed in the first set. This alternate approach, which does not involve repeated couplings of the GCM and ice-sheet model, was used for the sole reason that it was less computationally intensive. In comparisons of our coupled and uncoupled methods, we found no differences in whether ice sheets were initiated, justifying use of the uncoupled method in this inception analysis (see the Data Repository). These experiments were conducted with 1120 ppm $pCO_2$ and both a constant solar luminosity (97.5% of modern) and age-dependent solar luminosity (Gough, 1981), and with 2240 ppm $pCO_2$ (8× $CO_2$) using age-dependent solar luminosity. Luminosity was calculated by reducing the modern by ~1% per 100 m.y. after Crowley and Baum (1992).

Other than the parameters described here, all other boundary conditions were identical between experiments. To promote ice sheet initia-

*E-mail: dplowry@umich.edu.

[1]GSA Data Repository item 2014232, detailed methods and discussion, supported by four supplemental figures, is available online at www.geosociety.org/pubs/ft2014.htm, or on request from editing@geosociety.org or Documents Secretary, GSA, P.O. Box 9140, Boulder, CO 80301, USA.

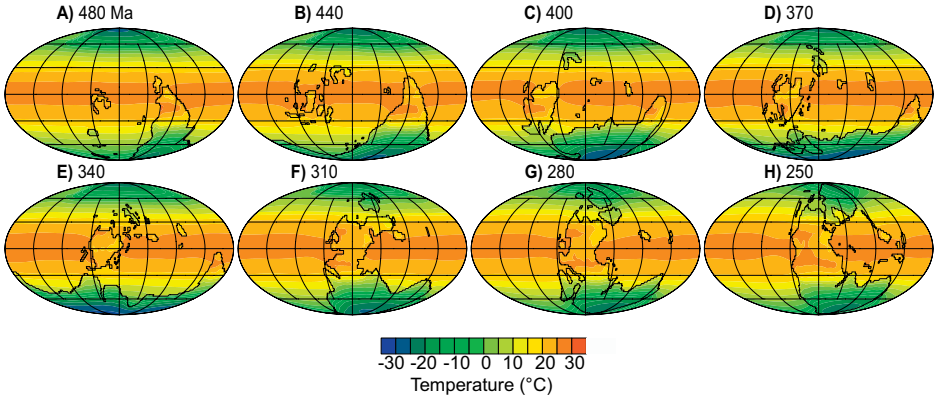


**Figure 1. Paleogeographic configuration and simulated mean annual temperature (°C) at 2× $CO_2$ (Cocks and Torsvik 2002; Torsvik and Cocks 2004). A: Early Ordovician (480 Ma). B: Early Silurian (440 Ma). C: Early Devonian (400 Ma). D: Late Devonian (370 Ma). E: Early Carboniferous (340 Ma). F: Late Carboniferous (310 Ma). G: Early Permian (280 Ma). H: Early Triassic (250 Ma).**

tion, orbital parameters representative of a cold Southern Hemisphere summer were specified by selecting parameter values from the past 10 m.y. (obliquity at 22.079°; eccentricity at 0.057133; precession at 270°; Berger and Loutre, 1991). Atmospheric trace gas concentrations were set to pre-industrial values ($CH_4$ 0.650 ppm; $N_2O$ 0.285 ppm; chlorofluorocarbons 0 ppb). Due to substantial paleotopographic uncertainties and our desire to isolate the effects of landmass distribution on ice sheet initiation, we utilize a 500 m uniform topography for each continental configuration.

## RESULTS

### Climate Prior to Ice-Sheet Coupling

To determine the response of the climate system to changes in the configuration of the continents, we compare the mean annual surface temperature (MAT) of each Paleozoic time slice from the initial GCM simulations prior to ice sheet-coupling. MATs are sensitive to both paleogeography and atmospheric $pCO_2$ (Figs. 1 and 2). At 2× $CO_2$, global MATs differ by as much as 2.7 °C between geographies, with early Carboniferous, Devonian, and Early Ordovician (340, 370, and 400 Ma, respectively) simulations having the lowest global MATs (12.7, 12.9, and 12.4 °C, respectively) and early Permian (280 Ma) and Early Triassic (250 Ma) simulations having the highest (14.7 and 15.1 °C, respectively).

Zonal-average MATs vary little between experiments at low latitudes (<0.6 °C between 30°N and 30°S), but show larger differences at high latitudes (~14.0 °C between 60° and 90°S and 12.3 °C between 60° and 90°N; Fig. 1). In the Southern Hemisphere, the lowest temperatures occur when landmasses are concentrated in high latitudes, while the opposite is true in the Northern Hemisphere (Fig. 1). The northward movement of continental blocks into the high mid-latitudes of the Northern Hemisphere, starting at 310 Ma, causes a doubling of total meridional heat transport due to the setup of strong seasonal temperature gradients between the land and ocean. Seasonal contrasts disrupt the zonal flow of winds and cause strong northerly surface winds in the summer, and southerly surface winds in winter, advecting cool air southward and warm air northward (see the Data Repository).

Global MAT differences between experiments with different continental configurations but identical $CO_2$ levels are primarily related to differences in albedo. Top-of-atmosphere shortwave radiation varies by ~5.4 $Wm^{-2}$, larger than differences in greenhouse forcing (~2.4 $Wm^{-2}$). Global MATs show a strong negative correlation with both planetary albedo ($R^2$ = 0.96) and surface albedo ($R^2$ = 0.98). Planetary and surface albedos are directly related to southern high-latitude (>60°S) land fractions because these landmasses tend to have annual snow cover.

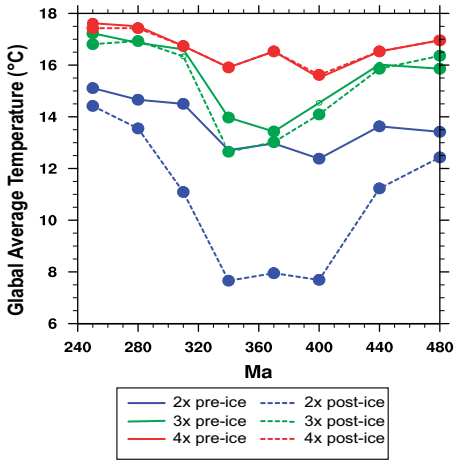


**Figure 2. Global mean annual surface temperatures (°C) prior to ice sheet simulation (solid lines) and after ice sheet simulation (dashed lines) for 2× $CO_2$ (blue line), 3× $CO_2$ (green line), and 4× $CO_2$ (red line).**

The global MAT response to increasing $pCO_2$ varies with geography (Fig. 2). Doubling $pCO_2$ from 2× to 4× $CO_2$ yields a global MAT increase of 3.0 °C, with a minimum increase of 2.5 °C at 250 Ma and a maximum increase of 3.6 °C at 370 Ma. Greenhouse forcing rises by 3.1–6.0 $Wm^{-2}$ between these experiments, and alone cannot account for the full temperature change. Positive feedbacks on snow and sea ice are larger than the direct greenhouse forcing, and increase the absorbed solar radiative forcing by 7.5–18.1 $Wm^{-2}$ between 2× and 4× $CO_2$ simulations.

### Ice Sheet Initiation

Continental ice sheets simulated using the asynchronous coupling technique initially form at high-latitude coastlines, expand inland, and continue to thicken until equilibrium with the imposed climate is reached at ~50,000 yr. All 2× $CO_2$ simulations produce substantial continental ice sheets on southern Gondwana, while trace amounts of coastal ice form in northern Laurasia, but do not contribute substantially to global ice volume (<1%). Increasing $pCO_2$ limits ice sheet formation by raising summer surface temperatures above freezing. At 3× $CO_2$, ice sheet initiation varies according to geography with mid-Paleozoic (400–310 Ma) simulations growing the largest ice sheets. At 4× $CO_2$, only trace amounts of coastal ice are simulated (Fig. 3).

Continental configurations influence ice sheet initiation by increasing the land area where freezing temperatures and precipitation coincide. The ice sheets do not initiate in the continental interior, despite cooler temperatures, because conditions are too arid due to a lack of precipitable moisture. Both land area and coastal length below 60°S latitude are positively correlated with ice volume, ice surface area, and snowfall. Large southern high-latitude landmasses at 400–340 Ma yield the lowest surface temperatures (Fig. 1), resulting in the largest simulated ice sheets (Figs. 3 and 4).

Continental configurations have different ice sheet initiation–$pCO_2$ thresholds. The $pCO_2$ threshold for substantial ice sheet initiation is <840 ppm in the 250, 280, 440, and 480 Ma cases. In the 310 and 400 Ma cases, the threshold is higher, between 840 and 1120 ppm (Fig. 3). At 4× $CO_2$, either no ice or very small coastal glaciers are simulated for all geographic configurations.

### Equilibrium Glacial Conditions

Equilibrium glaciation and atmospheric conditions were simulated using the asynchronous coupling technique (see the Methods discussion). Ice sheet volumes increase from their initial values by ~0.5–1.5 × $10^8$ $km^3$ (~200%–300%) at the 2× $CO_2$ level, ~0–1.4 × $10^8$ $km^3$ (~0%–600%) at the 3× $CO_2$ level, and 0–1.7 × $10^7$ $km^3$ (~0%–2100%) at the 4× $CO_2$ level. Small coastal glaciers simulated for cases at 3×

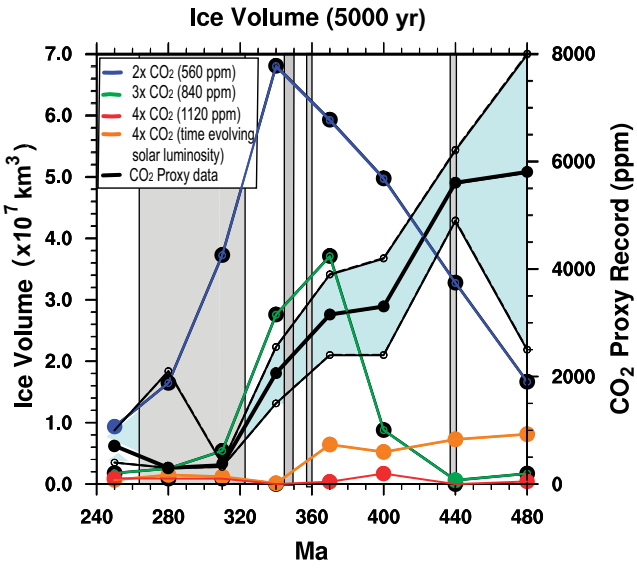


**Figure 3. Ice volume ($10^7$ km$^3$) after 5000 yr of ice sheet simulation for time slices during the Paleozoic at 2× $CO_2$ (blue line), 3× $CO_2$ (green line), and 4× $CO_2$ (red line) with constant solar luminosity, and 4× $CO_2$ with time-varying solar luminosity (orange line). Documented glacial events, which include the Late Ordovician, Late Devonian, early Carboniferous, and late Paleozoic glaciations, are indicated by gray shading (Brenchley et al., 2003; Caputo and Crowell, 1985; Fielding et al., 2008). Proxy record of atmospheric $CO_2$ is shaded in light blue. Solid black line represents the best estimate; dashed lines indicate the uncertainty (modified after Royer, 2006).**

and 4× $CO_2$ levels do not grow substantially and remain restricted to the coastlines. Simulated ice volume for 310 Ma is comparable to peak LPIA ice volume estimates (~13% larger; Fielding et al., 2008) at 2× $CO_2$ but is substantially lower at 3× $CO_2$ (~93% smaller).

Similar to initiation, geography influences equilibrium ice sheet size, as greater high-latitude land mass promotes ice sheet growth (Fig. 4). In particular, as Gondwana moved further southward over the pole from the Early Devonian (400 Ma) to the early Carboniferous (340 Ma), the footprint of simulated ice sheets expanded. Ice sheet size decreased as most of Gondwana drifted equatorward, colliding with northern Laurasia during the late Paleozoic (340–250 Ma).

In the 2× $CO_2$ experiments, the large expansion of continental ice reduces global average temperature by 0.7–5.0 °C due to concomitant increases in surface albedo and ice sheet elevation (Fig. 2). The temperature change is largest at high latitudes (~9.3–14.5 °C between 60° and 90°S and ~6.1–7.8 °C between 60° and 90°N), with little change at low latitudes (<0.7 °C between 30°S and 30°N). In comparison to the 2× $CO_2$ experiments, MATs in the 4× $CO_2$ experiments are 3.0–8.6 °C higher, with an average of 5.9 °C, demonstrating the large temperature response to ice sheet feedbacks (Fig. 2).

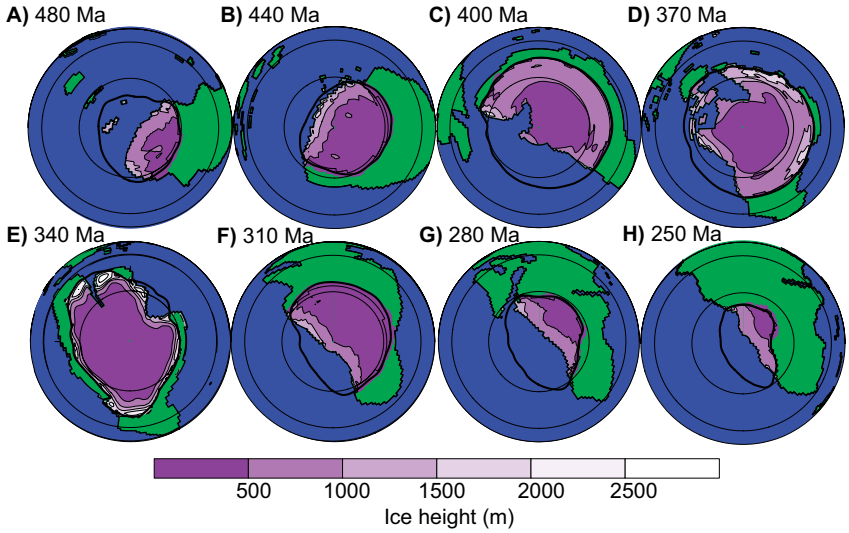


**Figure 4. Polar projection maps of Southern Hemisphere simulated Paleozoic ice sheet heights (m) at 2× $CO_2$ with Southern Hemisphere cold summer (SHCS) orbital configuration for eight Paleozoic time slices. Heights represent equilibrium ice sheet conditions after 50,000 yr of model integration (see text for details). Latitude is shown at 30° intervals (thin black lines). The 0° C isotherm for January (Southern Hemisphere summer) is indicated by the thick black isotherm. Note that ice heights are greatest near coastlines. Unglaciated land surfaces are shown in green, and ocean is shown in blue.**

### Sensitivity to Solar Luminosity

Accounting for solar evolution increases ice sheet volumes in the earlier Paleozoic when luminosity was lowest. In the 4× $CO_2$ simulations, ice sheet volumes for time slices between 480 and 370 Ma are substantially greater than those simulated with constant luminosity (Fig. 3). At 8× $CO_2$, the total ice volume is small or nonexistent in all simulations; only trace amounts of continental ice form along the coastlines at 400 Ma and 480 Ma. These results suggest that the threshold $pCO_2$ level for glacial inception decreased through the Paleozoic from a high near 4× $CO_2$ in the early Paleozoic to a value near 2× $CO_2$ in the late Paleozoic.

## DISCUSSION

Our coupled GCM–ice sheet model results indicate that neither continental drift nor time-appropriate solar luminosity is able to explain the geologic history of Paleozoic glaciation. In contrast to the geologic record, our late Paleozoic simulations (310 and 280 Ma) show significantly less continental ice than our early Paleozoic simulations, indicating that other factors were responsible for widespread glaciation. The most favorable geographic configurations for ice formation are those of the mid-Paleozoic (400 and 340 Ma), when Gondwana migrated over the austral pole (Figs. 3 and 4). This interval coincides with the Late Devonian and early Carboniferous glaciations, and suggests that ice sheet formation was facilitated by favorable geographic configurations. However, continental configurations do not explain why these events were brief in duration or why the majority of this interval remained ice free.

Our modeling results are consistent with the geologic record when atmospheric $pCO_2$ is taken into account, indicating that $pCO_2$ was likely a primary control on Paleozoic glaciation. According to the $pCO_2$ proxy record, the mainly ice-free early and mid-Paleozoic coincide with high $pCO_2$ concentrations (≥1120 ppm) and the LPIA coincides with low $pCO_2$ concentrations (≤560 ppm; Royer, 2006). Under constant solar luminosity, we simulate continental-scale ice sheets at 2× $CO_2$, but above this threshold, substantially less ice forms (Fig. 3). This result is consistent with proxy evidence of covariance between LPIA ice volume and $pCO_2$ (Montañez et al., 2007). Early Paleozoic solar luminosities raise the $pCO_2$ threshold to 4× $CO_2$; however, this threshold remains too low to explain the short-lived Late Ordovician glaciation, which is thought to have occurred at $pCO_2$ of >8× $CO_2$ (Herrmann et al., 2003; Young et al., 2010). However, it has been hypothesized that the temporal resolution of the proxy record remains too coarse to capture short-term variations in deep-time $pCO_2$. For example, Young et al. (2010) reported trends in carbonate and marine organic matter $\delta^{13}C$ that suggest dynamic, short-lived

atmospheric $pCO_2$ fluctuations during the Late Ordovician (Hirnantian) glacial interval.

A limitation of our study is the application of uniform topography in our simulations. High topography can act as an ice nucleation center and modify atmospheric heat transport and precipitation through its influence on stationary wave patterns (e.g., Fiorella and Poulsen, 2013), each of which could affect $pCO_2$–ice sheet initiation thresholds. We also note that in the absence of topography, our simulated ice sheets flow from the coast to the interior of the continents, at odds with the glacial sedimentary record (e.g., Fielding et al., 2008) and in contrast to LPIA ice sheet simulations in which topographic variations are included (e.g., Horton et al., 2007, 2010). We emphasize that our results focus on thresholds for continental-scale ice sheet initiation and are not intended for basin-scale comparison.

Our results suggest that continental drift does not directly drive glaciation. However, our simulations do not include tectonic–carbon cycle feedbacks, leaving open the possibility that continental drift indirectly drove glaciation by influencing atmospheric $pCO_2$. Goddéris et al. (2014) reported that enhancement of silicate weathering on warm, moist low-latitude continents can initiate glaciation. In our simulations, we observe an increase in tropical continental precipitation between 30°S and 30°N in the 480–310 Ma interval that may have facilitated lower atmospheric $pCO_2$. However, the formation and uplift of Pangaea leads to widespread aridity, suggesting that this mechanism is unlikely to explain the late Paleozoic glaciation.

A number of studies have recently estimated past Earth system sensitivity, the long-term response of global average temperature to doubled $pCO_2$ considering both fast ($<10^2$ yr) and slow ($>10^3$ yr) climate feedbacks, in order to constrain future climate sensitivity (cf. Royer et al., 2012). Paleoclimate data show a sensitivity of ~3 °C when considering fast climate feedbacks on short time scales, but as much as 6 °C when slow climate feedbacks, such as glacial-interglacial cycles, are also considered (Royer et al., 2012). Our Earth system sensitivity estimates for the Paleozoic range from 3.0 °C to 8.6 °C, depending on the size of the resulting ice sheet. This result indicates that Earth system sensitivities change as a function of continental configuration, consistent with previous modeling studies (e.g., Goddéris et al., 2014), and suggests that using past Earth system sensitivities to infer modern or future ones is imprudent.

## CONCLUSIONS

We contend that atmospheric $pCO_2$ is the primary control on Paleozoic glacial inception, but that changes in landmass configuration and solar luminosity modify $pCO_2$ glacial inception thresholds. $pCO_2$ glacial inception thresholds may have been as low as 560 ppm (2× $CO_2$) in the late Paleozoic but as high as 1120 ppm (4× $CO_2$) in the earliest Paleozoic due to lower solar luminosity and differences in continental geography. Our results suggest that climate sensitivity is nonstationary, with continental drift playing a primary role in its evolution through time.


## ACKNOWLEDGMENTS

We thank C. Fielding and two anonymous reviewers for comments on this manuscript. This research was supported by the National Science Foundation (grant EAR-1338200).


## REFERENCES CITED


Alder, J.R., Hostetler, S.W., Pollard, D., and Schmittner, A., 2011, Evaluation of a present-day climate simulation with a new coupled atmosphere-ocean model GENMOM: Geoscientific Model Development, v. 4, p. 69–83, doi:10.5194/gmd-4-69-2011.

Berger, A., and Loutre, M.F., 1991, Insolation values of the last 10 million years: Quaternary Science Reviews, v. 10, p. 297–317, doi:10.1016/0277-3791(91)90033-Q.

Brenchley, P.J., Carden, G.A., Hints, L., Kaljo, D., Marshall, J.D., Martma, T., Meidla, T., and Nõlvak, J., 2003, High-resolution stable isotope stratigraphy of Upper Ordovician sequences: Constraints on the timing of bioevents and environmental changes associated with mass extinction and glaciation: Geological Society of America Bulletin, v. 115, p. 89–104, doi:10.1130/0016-7606(2003)115<0089:HRSISO>2.0.CO;2.

Caputo, M.V., and Crowell, J.C., 1985, Migration of glacial centers across Gondwana during Paleozoic Era: Geological Society of America Bulletin, v. 96, p. 1020–1036, doi:10.1130/0016-7606(1985)96<1020:MOGCAG>2.0.CO;2.

Cocks, L.R.M., and Torsvik, T.H., 2002, Earth geography from 500 to 400 million years ago: A faunal and palaeomagnetic review: Geological Society of London Journal, v. 159, p. 631–644, doi:10.1144/0016-764901-118.

Crowley, T.J., and Baum, S.K., 1992, Modeling late Paleozoic glaciation: Geology, v. 20, p. 507–510, doi:10.1130/0091-7613(1992)020<0507:MLPG>2.3.CO;2.

Fielding, C.R., Frank, T.D., Birgenheier, L.P., Rygel, M.C., and Jones, A.T., 2008, Stratigraphic imprint of the late Paleozoic ice age in eastern Australia: A record of alternating glacial and nonglacial climate regime: Geological Society of London Journal, v. 165, p. 129–140, doi:10.1144/0016-76492007-036.

Finnegan, S., Bergmann, K., Eiler, J.M., Jones, D.S., Fike, D.A., Eisenman, I., Hughes, N.C., Tripati, A.K., and Fischer, W.W., 2011, The magnitude and duration of Late Ordovician–Early Silurian glaciation: Science, v. 331, p. 903–906, doi:10.1126/science.1200803.

Fiorella, R.P., and Poulsen, C.J., 2013, Dehumidification over tropical continents reduces climate sensitivity and inhibits snowball Earth initiation, Part I: Climate dynamics: Journal of Climate, v. 26, p. 9677–9695, doi:10.1175/JCLI-D-12-00820.1.

Goddéris, Y., Donnadieu, Y., Le Hir, G., Lefebvre, V., and Nardin, E., 2014, The role of palaeogeography in the Phanerozoic history of atmospheric $CO_2$ and climate: Earth-Science Reviews, v. 128, p. 122–138, doi:10.1016/j.earscirev.2013.11.004.

Gough, D.O., 1981, Solar interior structure and luminosity variations: Solar Physics, v. 74, p. 21–34, doi:10.1007/BF00151270.

Herrington, A.R., and Poulsen, C.J., 2012, Terminating the Last Interglacial: The role of ice sheet–climate feedbacks in a GCM asynchronously coupled to an ice sheet model: Journal of Climate, v. 25, p. 1871–1882, doi:10.1175/JCLI-D-11-00218.1.

Herrmann, A.D., Patzkowsky, M.E., and Pollard, D., 2003, Obliquity forcing with 8–12 times preindustrial levels of atmospheric $pCO_2$ during the Late Ordovician glaciation: Geology, v. 31, p. 485–488, doi:10.1130/0091-7613(2003)031<0485:OFWTPL>2.0.CO;2.

Horton, D.E., Poulsen, C.J., and Pollard, D., 2007, Orbital and $CO_2$ forcing of late Paleozoic continental ice sheets: Geophysical Research Letters, v. 34, p. L19708–L19713, doi:10.1029/2007GL031188.

Horton, D.E., Poulsen, C.J., and Pollard, D., 2010, Influence of high-latitude vegetation feedbacks on late Paleozoic glacial cycles: Nature Geoscience, v. 3, p. 572–577, doi:10.1038/ngeo922.

Kennett, J.P., 1977, Cenozoic evolution of Antarctic glaciation, the circum-Antarctic Ocean, and their impact on global paleoceanography: Journal of Geophysical Research, v. 82, p. 3843–3860, doi:10.1029/JC082i027p03843.

Montañez, I.P., and Poulsen, C.J., 2013, The late Paleozoic ice age: An evolving paradigm: Annual Review of Earth and Planetary Sciences, v. 41, p. 629–656, doi:10.1146/annurev.earth.031208.100118.

Montañez, I.P., Tabor, N.J., Niemeier, D., DiMichele, W.A., Frank, T.D., Fielding, C.R., Isbell, J.L., Birgenheier, L.P., and Rygel, M.C., 2007, $CO_2$-forced climate and vegetation instability during late Paleozoic deglaciation: Science, v. 315, p. 87–91, doi:10.1126/science.1134207.

Royer, D.L., 2006, $CO_2$-forced climate thresholds during the Phanerozoic: Geochimica et Cosmochimica Acta, v. 70, p. 5665–5675, doi:10.1016/j.gca.2005.11.031.

Royer, D.L., Pagani, M., and Beerling, D.J., 2012, Geobiological constraints on Earth system sensitivity to $CO_2$ during the Cretaceous and Cenozoic: Geobiology, v. 10, p. 298–310, doi:10.1111/j.1472-4669.2012.00320.x.

Torsvik, T.H., and Cocks, L.R.M., 2004, Earth geography from 400 to 250 Ma: A paleomagnetic, faunal and facies review: Geological Society of London Journal, v. 161, p. 555–572, doi:10.1144/0016-764903-098.

Young, S.A., Saltzman, M.R., Ausich, W.I., Desrochers, A., and Kaljo, D., 2010, Did changes in atmospheric $CO_2$ coincide with latest Ordovician glacial-interglacial cycles?: Palaeogeography, Palaeoclimatology, Palaeoecology, v. 296, p. 376–388, doi:10.1016/j.palaeo.2010.02.033.



Manuscript received 26 February 2014
Revised manuscript received 7 May 2014
Manuscript accepted 11 May 2014

Printed in USA